RSC Advances

Enhanced hydrophilic and antifouling polyacrylonitrile membrane with polydopamine modified silica nanoparticles

Journal:	*RSC Advances*
Manuscript ID	RA-ART-10-2015-022160.R1
Article Type:	Paper
Date Submitted by the Author:	14-Dec-2015
Complete List of Authors:	Tripathi, Bijay; Leibniz Institute of Polymer Research Dresden, Department of Nanostructured Materials Dubey, Nidhi; Leibniz Institute of Polymer Research Dresden, Germany, Subair, Riyas; Leibniz Institute of Polymer Research Dresden, Department of Nanostructured Materials; MG university, school of chemical sciences Choudhury, Soumyadip; Leibniz Institute of Polymer Research Dresden, Department of Nanostructured Materials; Technische Universität Dresden, Department of Chemistry Stamm, Manfred; Leibniz Institute of Polymer Research dresden
Subject area & keyword:	Films/membranes < Materials

Enhanced hydrophilic and antifouling polyacrylonitrile membrane with polydopamine modified silica nanoparticles

Bijay P. Tripathi,[a*] Nidhi C. Dubey, [a,b] Riyas Subair,[a] Soumydip Choudhury,[a] Manfred Stamm[a,b]

[a]*Department of Nanostructured Materials, Leibniz Institute of Polymer Research Dresden, Hohe Str. 6, D-01069 Dresden, Germany.*

[b]*Technische Universität Dresden, Department of Chemistry, Dresden 01069, Germany.*

Tel: +49-3514658652; Fax: +49-3514658281; E-mail: tripathi@ipfdd.de; bijayptripathi@yahoo.com

A simple and straightforward method for preparing hydrophilic and antifouling ultrafiltration membranes is described. Silica nanoparticles were synthesized and modified by mussel inspired dopamine polymerization. The ultrafiltration membranes were prepared using polyacrylonitrile (PAN) with different ratios of polydopamine modified silica nanoparticles (SiO_2-DOPA) via a phase inversion process. Composite membranes containing increasing amounts of SiO_2-DOPA were compared to the pure PAN membranes to determine the changes in performance, hydrophilicity, and antifouling characteristics. The composite membranes exhibited higher water permeation and rejection properties compared to those of the neat PAN membrane. During flux decline and recovery experiments, PAN-SiO_2-DOPA composite membranes exhibited higher flux recovery than a neat PAN membrane. The best performing membrane recovers more than 75% of its original flux after being washed with deionized water, demonstrating a high resistance to irreversible fouling. The composite membranes were tested for rejection of protein and dye molecules, and the high rejection efficiency with moderately declined fluxes indicates their suitability for separation and water treatment applications.

Keywords: *Polydopamine, silica nanoparticle, polyacrylonitrile, antifouling, rejection, water purification*

1. Introduction

The increasing application of membrane based technologies in various fields, such as the food and dairy industry, separation and purification technology, medical, catalysis and environmental remediation, desalination and water treatment, etc. led to an increased focus in recent past.[1-7] For all these applications highly porous, antifouling, tunable, and permeable membranes are required. Current membrane based filtration processes, such as ultrafiltration (UF), suffers with long-term operation due to the low resistance of the membranes to fouling. Membrane fouling, caused by the adsorption, accumulation, and growth of various organic, inorganic, and biofoulants on a membrane surface or in a membrane matrix during filtration,[8-10] results in reduced productivity, additional operating costs, and the need for frequent chemical cleaning that shortens membrane lifespan.[11-14] Thus, there is an urgent need to develop membranes with better anti-fouling property and stability as well as higher water flux for the above discussed membrane based processes.

Polyacrylonitrile (PAN) is one of the most promising and widely used membrane forming materials due to its outstanding properties such as high solvent resistance, chemical stability, thermal stability, mechanical strength, and membrane forming ability.[15-21] Like most of the membranes, PAN membranes are also prone to fouling leading to a shorter lifespan. Extensive efforts have been rendered to improve the antifouling property by improving the hydrophilicity through a variety of methods such as chemical treatment, surface grafting, and additive blending.[15, 16, 20, 22-24] These chemical treatments and grafting modification methods require numerous post-treatment processes which complicates the membrane preparation as well as

decreases the mechanical strength and performance. On the other hand the additive blending method often needs amphiphilic copolymers and inorganic nanoparticles.[16, 25-28] Among the various types of nanoparticles that are being used for addition to polymeric membranes are Al_2O_3, SiO_2, ZrO_2, TiO_2, Fe_3O_4, halloysite nanotubes, montmorillonite, carbon nanotubes, Ag, Au, zero valent iron (Fe^0), and Pd etc.[15, 29-33] These mixed membranes, where nanoparticles are blended in the polymeric membranes are expected to have a composite structure and to combine the basic properties of polymers and inorganic particles. The composite behavior with nanoparticles enhances the permeability, separation performance, antifouling property, and stability.

Fabricating polymeric membranes with various metal oxide nanoparticles is one of the most used methods to prepare composite membranes, because metal oxides can provide specific functionalities to the membrane, while retaining the intrinsic separation performance of the bare membrane. SiO_2 is one of the widely used inorganic nanoparticles in membrane fabrication because of its stability, good hydrophilicity, mild reactivity, and excellent resistance against chemicals.[15] PAN-SiO_2 composite membranes have been reported with improved porous structure and hydrophilicity.[15, 34, 35] However, the low miscibility between polymer and nanoparticles, because of the different surface properties of the two components, makes it difficult to achieve a highly dispersed nanocomposite membrane by direct blending.[15] The low miscibility and dispersion leads to nanoparticle aggregation. Therefore, SiO_2 nanoparticles should be suitably surface-modified to improve their compatibility with PAN and dispersion in PAN matrix. Surface modifications of SiO_2 nanoparticles by chemical bonding or physically adsorbing polymers are the most common methods to obtain hybrid nanoparticles.[15, 36, 37] In most of these modification approaches, complicated chemical synthesis, solvent extraction, etc. are required, which makes the process less economical and productive. Recently, bio-inspired polydopamine

(DOPA) coatings have attracted great attention as a biomimetic polymer and universal surface modification agent for various materials with a broad range of applications.[38-40] The DOPA polymerization occurs in weak alkaline aqueous media and very adherent polymer coatings on most organic and inorganic surfaces are formed.[41, 42] This modification approach is also used to modify different inorganic surfaces and nanoparticles.[43] DOPA modification also increases the hydrophilicity and tunability of the substrate due to multifunctional groups (amino and catechol groups).

Herein we report the fabrication of highly hydrophilic and antifouling membranes by using DOPA modified silica nanoparticles with PAN. The effect and concentration of DOPA modified silica nanoparticles on membrane formation and properties were systematically studied to determine the direct effect of the nanoparticles on the physico-chemical properties of the membranes, such as hydrophilic character, water permeability, fouling resistance, and solute rejection ability.

2. Experimental Section

2.1. Materials

Polyacrylonitrile, dopamine, and all other chemicals were purchased from Sigma-Aldrich, Inc. (St. Louis, Missouri, USA) and used as received. Nonwoven polyester fabric support for the membrane preparation was kindly provided by Freudenberg Filtration Technologies, Germany. For all purpose Millipore water was used.

2.2. Synthesis of silica nanoparticles and polydopmine modification

Silica nanoparticles were synthesized by a modified Stöber method.[44] In brief, 455 mg of L-Arginin was first dissolved in 345 ml of water and then 25 ml of cyclohexane was added. The

solution was then heated to 60 °C under stirring. To this solution 18 mL of tetraethyl orthosilicate (TEOS) was added and stirred for 48 hours. After that, the cyclohexane was separated by a separating funnel and the suspension of silica particles was filled in a dialysis membrane tube. The membrane tube was kept overnight in deionized water under stirring to remove any unreacted species. This method results SiO_2 particles with 8.9 mg mL^{-1} concentration, which was further concentrated up to ~450 mg mL^{-1} in a rotary evaporator and used for further applications.

The synthesized silica nanoparticles were washed with deionized water and dispersed in 2 mg mL^{-1} dopamine [4-(2-aminoethyl)benzene-1,2-diol] solution dissolved in 10 mmol L^{-1} tris-HCl buffer solution (pH 8.5, tris = 2-amino-2-hydroxymethyl-propane-1,3-diol). The particles were shaken for 24h at room temperature to obtain a DOPA layer coating on the surface. Finally, the DOPA coated silica nanoparticles were washed several times with deionized water by repeated dispersion and centrifugation. Washed nanoparticles were dried in a vacuum oven and used for membrane preparation.

2.3. Membrane preparation

Composite PAN based membranes containing different amount of modified silica nanoparticles were fabricated via the immersion precipitation method. First a 10 wt.% PAN solution was prepared in *N,N*'-dimethylformamide (DMF) and filtered through a 0.45 μm PTFE filter. The dopamine modified silica nanoparticles were dispersed separately in DMF by ultra-sonication and PAN solution was added drop wise into this dispersion under stirring. The concentration of PAN solution was maintained in such a way that the final solution concentration to be 10 wt.% and the particle content was varied from 5 wt. to 15 wt. %. The membranes were cast using a doctor blade at 150 μm gate height on a non-woven polyester fabric support wetted with DMF and taped to a glass plate. After being cast, the glass plate was immersed in a coagulation bath containing

water and ethanol in 70/30 ratio. The membrane was kept in the coagulation bath for 1 h and then transferred to a deionized water bath for 24 h to remove any residual solvent. Finally, the membranes were washed and stored in deionized water at room temperature. The membranes were denoted as PAN, PAN-SiO_2-5%, and PAN-SiO_2-DOPA-X% (where X is 5, 10, and 15%) for neat membrane, membrane with unmodified silica nanoparticles, and dopamine modified nanoparticle containing membranes, respectively.

2.4. Characterizations

The water uptake was determined gravimetrically after soaking the fully dried membrane samples in deionized water for 24 h. After wiping out the surface water, membranes wet weight was again recorded and the percent water uptake was calculated based on the weight change to that of the dry membrane.[45] The porosity of the membranes was calculated as a function of membrane weight before and after water absorption.[29] Films of known area and dry weight were immersed in deionized water for 24 h prior to measurement of swelling state. The porosity was calculated using the following equation:

$$Porosity\ (\%) = \left(\frac{W_w - W_d}{S d \rho} \right) \times 100 \qquad (1)$$

where W_w and W_d are the wet and dry weights of the membranes, respectively; S the membrane area; d the thickness and ρ is the density of water. The water uptake and porosity data were the average values obtained for 3 samples of each membrane.

The hydrophilic behavior of the membranes was studied employing the optical contact angle measurement system OCA40 (Data Physics, Bad Vilbel, Germany). Contact angles were measured by sessile drop experiments as reported earlier using deionized water (surface tension of 72.8 mN m^{-1}).[8, 39] The variation in the measured contact angle values was within ±2°, and the

values reported are averages of at least three measurements from three different membrane samples. The free energy values of the solid-liquid interface ($-\Delta G_{sL}$) were calculated from the advancing contact angle values using a water surface tension value of 72.8 mJ m^{-2}.[39, 46]

The surface and cross-section morphologies of dried samples were observed using a NEON 40 FIB-SEM workstation (Carl Zeiss AG, Germany) operated at 3 kV, after 3 nm thick sputter coating of platinum. Cross-section images were obtained after breaking the membranes in liquid nitrogen. The contact angle of membranes was measured with optical contact angle measurement system (Data Physics OCA40, Germany) using sessile drop method at five places on same membrane.

2.5. Protein and dye adsorption

Fouling of the membrane surfaces was characterized by BSA and Congo red adsorption under shaking condition at room temperature. The membranes with known dry weight and area were presoaked in deionized water for 24 h and then kept in respective dye and protein solution under gentle shaking for 6 h. The amount of dye and protein adsorption was estimated by recording the change in absorbance of the solution to that of original solution in UV-vis spectroscopy. The amount of adsorbed BSA and dye was calculated using following Equation:

$$R = \left(1 - \frac{C_R}{C_O}\right) \times 100 \qquad (2)$$

where C_R and C_O is the remaining and the initial concentration of protein/dye in the solution, respectively.

2.6. Water flux, rejection, and flux recovery studies

The hand-cast membranes with nonwoven support were used for pure water permeability and flux decline during rejection and recovery studies. To determine the pure water permeability values a Millipore dead end filtration device connected with a nitrogen gas cylinder and solution reservoir was used. The membranes were first compacted with deionized water at 3.5 bar until the flux was stabilized. The stable flux was recorded as the pure water permeability at varying pressures from 0.5 to 3 bar. The pure water flux (J_w) was calculated by the following equation:

$$J_w = \frac{Permeate\ volume\ (L)}{Area\ (m^2) \times Time\ (h)} \qquad (3)$$

The rejection performance was evaluated using BSA protein and Congo red dye in triplicate from the same batch of membrane from three different regions. The solutions were filtered in the dead end filtration device and the rejection was estimated based on change in concentration. Filtrate samples were collected after reaching the steady state flux under vigorous stirring condition. The concentration of solutes in the feed and permeate was obtained with the help of UV-vis spectroscopy. The rejection (R) was calculated using the following equation:

$$R = \left(1 - \frac{C_p}{C_f}\right) \times 100 \qquad (4)$$

where C_p and C_f are permeate and feed concentrations of solutes, respectively. Flux recovery was also estimated for the prepared membranes to analyze the flux decline and recovery testing. Solutions were charged in the filtration device with a membrane at stable water permeability and to observe the flux decline caused by solute adsorption (fouling). After obtaining again a stable flux, deionized water was introduced to wash the membrane surface. After proper washing, flux recovery was recorded when a stable flux was reached. The flux recovery (FR) was calculated via following equation:

$$FR(\%) = \frac{J_v}{J_w} \times 100 \qquad (5)$$

Where J_w and J_v are the deionized water fluxes before and after the fouling with solutes.

3. Results and Discussion

3.1. Silica nanoparticle modification and membrane fabrication

The uniform sized silica nanoparticles were synthesized by Stöber method. The preparation steps and its characterizations are presented in **Figure 1**. In a mixture of L-Arginine and cyclohexane solution, 18 ml of TEOS was added and stirred for 48 h which yielded ~70% of SiO_2. The silica nanoparticles were modified by mussel inspired polydopamine modification by dispersing in a dopamine solution (prepared in 10 mmol L^{-1} tris-HCl buffer solution) under vigorous shaking condition for 24 h at room temperature. The schematic of DOPA modification of silica nanoparticles is represented in Figure 1 **(A)**. After that the particles were washed with deionized water by centrifugation and redispersion till clear supernatant solution. The hydrodynamic size of neat and modified silica nanoparticles was found to be 19 and 24 nm, respectively (**Figure 1 (B)**).Thus obtained DOPA modified silica nanoparticles were dried in vacuum oven at 60 ^oC and used for membrane preparation. **Figure 1 (C and D)** shows the SEM images of neat and DOPA modified silica nanoparticles. Compared with the silica nanoparticles with an average diameter of 20 nm, the diameter of SiO_2-DOPA was found to be about 25 nm. This indicates that ca. 5 nm thin DOPA layer was successfully formed on the surface of silica nanoparticles through the oxidative self-polymerization of the dopamine. It can also be seen in the image that the DOPA modified nanoparticles were tending to agglomerate or joined together due to DOPA film.

The DOPA modification of nanoparticles was also characterized by studying the thermal degradation pattern in N_2 environment. The TGA data are presented in **Figure 2 (A)**. The initial

weight loss in case of SiO_2-DOPA indicates desorption of water as well as the degradation of organic DOPA part. However, in same ranges a higher weight loss for neat silica nanoparticle shows the water loss and degradation of surfactant used during its preparation. The degradation pattern for SiO_2-DOPA after 500 ^oC, shows the complete degradation of DOPA layer.

The nanocomposite membranes were prepared using unmodified and DOPA modified silica nanoparticles with PAN as membrane forming material by solution casting and non-solvent phase inversion method. The step-wise approach for membrane preparation is depicted in **Figure 3**. First the nanoparticles were dispersed in DMF by stirring and ultra-sonication. This nanoparticle dispersion was then mixed with an already prepared PAN solution and stirred for 24 h. The DOPA modification of silica nanoparticles resulted in better dispersion in organic solvent during membrane formation. Large numbers of amine functional groups on polydopamine layer also make it more compatible to PAN polymer matrix. The SiO_2-DOPA particles were well dispersed in PAN solution and no sedimentation or agglomeration of particles was observed when stored for longer time. This indicates that there was a good compatibility between DOPA modified silica nanoparticles and PAN matrix. The final membrane forming solution was then allowed to degas for some time to remove any trapped air bubbles. The membranes were then cast on the solvent wetted non-woven fabric and solvent was allowed to evaporate for 60 s. Then the film was transferred to the solvent bath for phase inversion and washed several times with deionized water to remove the organic solvent from the membrane. The membranes were prepared with varying SiO_2-DOPA content (5, 10 and 15%) to study its effect on membrane properties.

3.2. Membrane morphology and hydrophilic properties

Figures 4-6 show the SEM images of the surface and cross-section morphology of control and nanocomposite membranes. The images indicate that the DOPA modification and the nanoparticles concentration in membrane forming solution have a clear effect on the membrane structure, which can be described in terms of silica nanoparticle agglomerations, pore size, porosity, and hydrophilic behaviors. The high polymer fraction leads to the formation of a denser upper layer during phase inversion due to faster drying of solvent and less interaction with water molecules. The presence of modified silica particles enhances the hydrophilicity of the film and a stronger interaction with water molecules during the phase inversion process which led to the formation of highly porous membrane with macrvoids in the matrix. Membrane prepared with unmodified silica nanoparticles (**Figure 4 (B))** shows high exclusion from the membrane matrix. This may be due to the release of hydrophilic nanoparticles from a relatively hydrophobic phase during phase inversion. It also indicates a low nanoparticle-polymer interaction. It is well known that oxide nanomaterials show a tendency to aggregate due to their high specific surface area and hydroxide groups on the surface.[29, 47] The surface modification of these nanoparticles reduces aggregation and enhances their dispersion in solution.[48] In our case, the polydopamine modification of silica nanoparticles led to the formation of homogeneous dispersed nanocomposite membranes even at high concentrations of nanoparticles. This may be due to the increased interaction between DOPA modified silica nanoparticles and PAN matrix. Membranes with DOPA modified silica nanoparticles shows less aggregation as compared to unmodified ones. Also no exclusion of nanoparticles from membrane matrix occurred. **Figure 4 (C and D)** with low nanoparticle content (5 and 10%) shows almost smooth surface along with a finger like macrovoids (**Figure 4 (E**)) distributed all through the membrane matrix. **Figures 5 and 6** represent the surface and cross-section images of PAN-SiO_2-DOPA-15% membrane. The surface of the membrane is relatively smoother and contains some agglomeration of particles but

no exclusion of nanoparticles from the membrane matrix. The cross-section images clearly indicate that big macrovoids together with small voids were formed in this case. The upper layer was relatively thin as compared to the other membranes which may be due to faster penetration of non-solvent and low drying rate. The high magnification of cross-section (Figure 6(E)) indicates that the macrovoids entered throughout the membrane and are separated with thin porous layers. The silica nanoparticles distribution can be clearly seen in the walls of macriovoids which make the membrane highly hydrophilic and less resistive towards water transport.

Table 1 summarizes the water absorption, contact angle, and porosity data of the prepared membranes. Among all prepared membranes, the neat PAN membrane showed lowest water absorption, porosity, and highest contact angle because of their relatively hydrophobic nature as compared to the prepared composite membranes. The hydrophilicity of the membranes increased with the inclusion of silica nanoparticles which was further enhanced by DOPA modification. A linear trend can be seen in the data with the increasing amount of doped silica nanoparticles. PAN-SiO_2-DOPA-15% showed highest water absorption and porosity. The increased water uptake can be attributed to the silica particles and DOPA modification which enhances the water binding capacity due to the presence of a large number of hydrophilic groups.

The porosity of all membranes was calculated based on the water uptake according to equation 1. As a result of the doping of nanoparticles the porosity of the membrane increases. This behavior can be attributed to the enhanced macrovoid formation leading to a higher membrane specific area which favors water sorption inside the membrane.[29, 45] Also, the initial drying time, coagulation bath temperature, coagulation solvent, and coagulation solvent-polymer interaction, etc. play an important role in overall porosity of the membrane. In this case, the coagulation solvent-polymer interaction was increased with the increasing hydrophilic silica

content in the membrane matrix which increases the hydrogen bonding capabilities between water and membrane matrix. The highest porosity was observed for PAN-SiO_2-DOPA-15% membrane which is ~20% more than for neat PAN membrane. This increase in porosity was due to high water absorption (>2.5 times as compared to the neat PAN membrane) and their retention due to the strong hydrogen bonding.

Contact angle values for all prepared membranes also show a similar trend as obtained for water absorption. The improved hydrophilicity with increased content of nanoparticles was evident with decreasing the contact angle value of the PAN membrane from 68^o for PAN to 32^o for PAN-SiO_2-DOPA-15% membrane. The increasing nanoparticle concentration favors solvent inter-diffusion and hence, the average pore size and porosity and leads to increase in the hydrophilicity. The work of adhesion (modulus of the interaction free energy ΔG_{SL}) resulting from interactions between the solid surface and the applied water molecules, was also increased with the amount of silica nanoparticles. These findings clearly indicate that the prepared membranes were highly hydrophilic and porous in nature which is required properties of filtration membranes.

3.3. Water permeation studies

Membrane permeation properties depend upon several parameters such as porosity, pore size, hydrophilicity, upper layer thickness, sublayer morphology, etc. The increased porosity and hydrophilicity lead to an increase in water permeability. Also, the membrane permeability is inversely proportional to the thickness of a membrane (especially the upper layer). The SEM images of prepared membranes indicate that the upper layer thickness was lowered with the increasing concentration of SiO_2-DOPA particles. The water absorption and contact angle data prove the highly hydrophilic nature of these membranes. Thus, from these aspects, the membrane

with 15% SiO_2-DOPA particles possesses all required properties for a high water permeating (i.e. low hydraulic resistance) membrane. The water permeation data of all membranes are shown in **Figure 7**.The flux of pure water increased significantly for nanocomposite membranes as compared to the neat PAN membrane. The enhancement was further improved with the DOPA modified particle inclusion in membranes as compared to the neat silica nanoparticles. PAN-SiO_2-DOPA-15% shows more than 10 times higher water flux than a neat PAN membrane.

The higher water permeation through nanoparticle containing membranes can be explained due to a higher affinity to water of SiO_2 and SiO_2-DOPA nanoparticles in comparison to the relatively hydrophobic PAN. The affinity of water towards SiO_2-DOPA should be even higher as compared to pure SiO_2 due to the presence of a large number of hydroxyl and amine functional groups. This affinity also affects the membrane morphology evolution and pore formation during the phase inversion process. The presence of nanoparticles, not only increases the water diffusion in membranes during the phase inversion, but also affects the polymer-solvent interaction.[29, 49] Thus the increased water permeation of SiO_2-DOPA containing membranes was a result of the increase in the membrane's porosity and hydrophilicity as well as the more open membrane structure, through the improvement in macrovoid formation.

3.4. Rejection properties

The rejection behavior of prepared membranes was evaluated using BSA protein and Congored dye in dead end filtration mode. The physical sieving phenomenon is believed to be one of the main driving forces which control the organic molecule rejection through filtration membranes. Additionally, the molecular size, charge nature, Donnan exclusion, the thickness of the membrane, hydrophilic/hydrophobic properties, and the degree of polymer swelling also influence the rejection properties. The rejection results along with the representative UV-vis

spectra for all membranes are presented in **Figure 8** (BSA) and **9** (Congo red). The rejection data indicate the typical molecular weight related rejection behavior. The membranes showed highest rejection for BSA because of to its high molecular weight and large molecular volume. The Congo red rejection was less than BSA which was obvious because of its low molecular weight. The rejection property of membranes was improved with the addition of SiO_2, and SiO_2-DOPA particles. The rejection was further improved with increasing concentration of SiO_2-DOPA in the membrane matrix. This increment in the rejection behavior can be explained due to the presence of entrapped nanoparticles in the pores and on the surface of the membranes. At higher concentration, the nanoparticles start plugging the pores of the membranes, causing an increase in the rejection of organic solutes.

3.5. Fouling and flux recovery studies

The presence of hydrophilic nanoparticles in the polymer membrane matrix enhances its overall hydrophilic behavior which has already been discussed above. This leads to a high surface hydration which is generally considered the key to nonspecific protein adsorption resistance, organic fouling, microorganisms attachment, etc., since a tightly bound water layer forms a physical and energetic barrier to prevent the adsorption to the surface.[8, 39, 45, 50-52] Considering that fouling is caused by adsorption of foulants on the membrane surface, the probability of BSA and Congo red dye adsorption was minimized due to the presence of nanosized hydrophilic SiO_2-DOPA particles. The relative BSA and Congo red adsorption on the prepared membranes is shown in **Figure 10**. The net adsorption for both compounds decreases with increasing nanoparticle concentration. Membrane showed relatively lower adsorption for BSA as compared to the Congo red. Due to the large size and high hydration, BSA molecules could not penetrate the membrane hydrophilic surface and thus a low adsorption was observed. Whereas, the Congo

red can diffuse inside the membrane pores due to its small size and gets entrapped, leading to a higher adsorption. This adsorption trend clearly indicates that the antifouling behavior of the membrane was improved by the addition of SiO_2-DOPA nanoparticles.

The fouling behavior of the prepared membranes was also studied under dynamic condition by repeated BSA protein filtration and washing of membrane surface and analyzing the flux recovery for each cycle. The flux recovery data can be used to indicate the reversible fouling properties of the membranes. The membranes which showed maximum flux recovery after proper washing are regarded as more antifouling and the fouling is considered as reversible fouling. **Figure 11** represents the first cycle of initial, with BSA, and recovered flux data of representative membranes, which clearly indicate that more than 75% flux was recovered in case of PAN-SiO_2-DOPA-15% membrane as compared to only 49% for neat PAN membrane. To further study the effect of washing and long-term recovery properties, the PAN and PAN-SiO_2-DOPA-15% membranes were subjected to a second and third cycle of protein filtration. The flux recovery data in second and third cycle for PAN was found to be 40 and 35.4% whereas for PAN-SiO_2-DOPA-15% membrane it was 73 and 71%, respectively. This observation clearly indicated that irreversible fouling occurred on the pure PAN membrane, while after the addition of SiO_2-DOPA nanoparticles, the flux decline was less significant, and the simple washing could effectively recover more than 70% of its initial permeation flux for continuous three cycles, indicating the improved antifouling performance of the nanocomposite membrane. These results could be attributed to the increased hydrophilicity of the membranes after the addition of SiO_2-DOPA nanoparticles, which decreased the affinity between the membrane surface and the proteins. In conclusion, the flux recovery data confirm the trend observed in adsorption and repeated BSA filtration studies which indicate the improved antifouling properties of the prepared nanocomposite membranes.

4. Conclusions

In summary, the mussel inspired DOPA modification of SiO_2 nanoparticles and its inclusion in PAN matrix was reported to obtain hydrophilic, low fouling, and high permeable membranes. A series of hybrid membranes with varying SiO_2-DOPA content was prepared by blending into the PAN matrix. The SiO_2 nanoparticle synthesis and its DOPA modification were well established by various characterization techniques. The DOPA modified nanoparticles were entrapped into the PAN matrix by solution dispersion and phase inversion process. The results showed that the SiO_2-DOPA nanoparticles could be well and homogeneously dispersed in the PAN matrix with low exclusion and agglomeration. The presence of DOPA on the surface of SiO_2 nanoparticles increases the compatibility with PAN matrix and therefore homogeneous dispersed nanocomposite membranes were formed. The mixing of SiO_2-DOPA nanoparticles also effectively improved the hydrophilicity, porosity, and water absorption properties. The microscopy images clearly proved the presence of nanoparticles in the membrane matrix and on the walls of the pores which reduces the water transport resistance which is reflected in high water transport through nanocomposite membranes. The presence of nanoparticles also enhanced the antifouling properties against protein adsorption. The nanocomposite membranes also showed improved rejection performance for BSA protein and Congo red dye. Furthermore, the high flux recovery of these membranes proved its long-term application. These properties indicate the usefulness of the PAN-SiO_2-DOPA membranes for water filtration and separation applications.

Acknowledgements

Authors acknowledge the funding by BMBF and DFG.

References

[1] A. Qin, X. Li, X. Zhao, D. Liu and C. He, *ACS Appl. Mater. Interf.*, 2015, **7**, 8427-8436.

[2] S. Liang, Y. Kang, A. Tiraferri, E. P. Giannelis, X. Huang and M. Elimelech, *ACS Appl. Mater. Interf.,* 2013, **5**, 6694-6703.

[3] A. Mohammad, C. Ng, Y. Lim and G. Ng, *Food Bioprocess Tech*, 2012, **5**, 1143-1156.

[4] M. A. Shannon, P. W. Bohn, M. Elimelech, J. G. Georgiadis, B. J. Marinas and A. M. Mayes, *Nature*, 2008, **452**, 301-310.

[5] M. Elimelech and W. A. Phillip, *Science*, 2011, **333**, 712-717.

[6] B. P. Tripathi, N. C. Dubey, S. Choudhury, F. Simon and M. Stamm, *J. Mater. Chem B*, 2013, **1**, 3397-3409.

[7] B. P. Tripathi, N. C. Dubey and M. Stamm, *ACS Appl. Mater. Interf.,* 2014, **6**, 17702-17712.

[8] B. P. Tripathi, N. C. Dubey, S. Choudhury and M. Stamm, *J. Mater. Chem.*, 2012, **22**, 19981-19992.

[9] B. P. Tripathi, N. C. Dubey and M. Stamm, *J. Hazard. Mater.*, 2013, **252-253**, 401-412.

[10] F. G. Meng, S. R. Chae, A. Drews, M. Kraume, H. S. Shin and F. Yang, *Water Res.*, 2009, **43**, 1489-1512.

[11] W. Chen, Y. Su, J. Peng, X. Zhao, Z. Jiang, Y. Dong, Y. Zhang, Y. Liang and J. Liu, *Environ. Sci. Technol.*, 2011, **45**, 6545-6552.

[12] Y.-H. Zhao, X.-Y. Zhu, K.-H. Wee and R. Bai, *J. Phys. Chem. B*, 2010, **114**, 2422-2429.

[13] D. Rana and T. Matsuura, *Chem. Rev.*, 2010, **110**, 2448-2471.

[14] A. Asatekin, S. Kang, M. Elimelech and A. M. Mayes, *J. Membr. Sci.*, 2007, **298**, 136-146.

[15] S.-H. Zhi, R. Deng, J. Xu, L.-S. Wan and Z.-K. Xu, *React. Funct. Polym.*, 2015, **86**, 184-190.

[16] C. Feng, J. Xu, M. Li, Y. Tang and C. Gao, *J. Membr. Sci.*, 2014, **451**, 103-110.

[17] I.-C. Kim, H.-G. Yun and K.-H. Lee, *J. Membr. Sci.*, 2002, **199**, 75-84.

[18] P. Ahmadiannamini, X. Li, W. Goyens, N. Joseph, B. Meesschaert and I. F. J. Vankelecom, *J. Membr. Sci.*, 2012, **394-395**, 98-106.

[19] Q.-Y. Wu, L.-S. Wan and Z.-K. Xu, *J. Membr. Sci.*, 2012, **409–410**, 355-364.

[20] H. R. Lohokare, M. R. Muthu, G. P. Agarwal and U. K. Kharul, *J. Membr. Sci.*, 2008, **320**, 159-166.

[21] A. Lu, A. Kiefer, W. Schmidt and F. Schüth, *Chem. Mater.*, 2004, **16**, 100-103.

[22] M. Ulbricht and G. Belfort, *J. Membr. Sci.*, 1996, **111**, 193-215.

[23] M. K. Sinha and M. K. Purkait, *RSC Adv.*, 2015, **5**, 66109-66121.

[24] M. K. Sinha and M. K. Purkait, *RSC Adv.*, 2015, **5**, 22609-22619.

[25] A. Adout, S. Kang, A. Asatekin, A. M. Mayes and M. Elimelech, *Env. Sci. Tech.*, 2010, **44**, 2406-2411.

[26] A. Asatekin, S. Kang, M. Elimelech and A. M. Mayes, *J. Membr. Sci.*, 2007, **298**, 136-146.

[27] Z.-Q. Huang, Z.-Y. Chen, X.-P. Guo, Z. Zhang and C.-L. Guo, *Ind. Eng. Chem. Res.*, 2006, **45**, 7905-7912.

[28] R. Saranya, G. Arthanareeswaran, S. Sakthivelu and P. Manohar, *Ind. Eng. Chem. Res.*, 2012, **51**, 4942-4951.

[29] A. Sotto, A. Boromand, S. Balta, J. Kim and B. Van der Bruggen, *J. Mater. Chem.*, 2011, **21**, 10311-10320.

[30] Q. Zhao, J. Hou, J. Shen, J. Liu and Y. Zhang, *J. Mater. Chem. A*, 2015, **3**, 18696-18705.

[31] S.A. Hashemifard, A.F. Ismail and T. Matsuura, *J. Colloid Interf. Sci*., 2011, **359**, 359-370.

[32] H. Yu, Y. Zhang, , X. Sun, J. Liu and H. Zhang, *Chem. Eng. J.*, 2014, **237**, 322-328.

[33] J. Zhu, M. Tian, Y. Zhang, H. Zhang and J. Liu, *Chem. Eng. J.*, 2015, **265**, 184-193

[34] H.-R. Jung, D.-H. Ju, W.-J. Lee, X. Zhang and R. Kotek, *Electrochim. Acta*, 2009, **54**, 3630-3637.

[35] J.-P. Lee, S. Choi and S. Park, *Nanoscale Research Letters*, 2012, **7**, 440-440.

[36] Y. Li and B. C. Benicewicz, *Macromolecules*, 2008, **41**, 7986-7992.

[37] Y. Huang, Q. Liu, X. Zhou, S. Perrier and Y. Zhao, *Macromolecules*, 2009, **42**, 5509-5517.

[38] H. Lee, S. M. Dellatore, W. M. Miller and P. B. Messersmith, *Science*, 2007, **318**, 426-430.

[39] B. P. Tripathi, N. C. Dubey, F. Simon and M. Stamm, *RSC Adv.*, 2014, 4, 34073-34083.

[40] Q. Ye, F. Zhou and W. Liu, *Chem Soc Rev*, 2011, **40**, 4244-4258.

[41] J. H. Waite, *Nat. Mater.*, 2008, **7**, 8-9.

[42] J. I. Clodt, V. Filiz, S. Rangou, K. Buhr, C. Abetz, D. Höche, J. Hahn, A. Jung and V. Abetz, *Adv. Funct. Mater.*, 2013, **23**, 731-738.

[43] X. Jia, M. Xu, Y. Wang, D. Ran, S. Yang and M. Zhang, *Analyst*, 2013, **138**, 651-658.

[44] K. D. Hartlen, A. P. T. Athanasopoulos and V. Kitaev, *Langmuir*, 2008, **24**, 1714-1720.

[45] B. P. Tripathi, N. C. Dubey and M. Stamm, *J. Membr. Sci.*, 2014, **453**, 263-274.

[46] G. R. Guillen, T. P. Farrell, R. B. Kaner and E. M. V. Hoek, *J. Mater. Chem.*, 2010, **20**, 4621.

[47] F. Aureli, M. D'Amato, B. De Berardis, A. Raggi, A. C. Turco and F. Cubadda, *J. Anal. At. Spectrom.*, 2012, **27**, 1540-1548.

[48] R. P. Bagwe, L. R. Hilliard and W. Tan, *Langmuir*, 2006, **22**, 4357-4362.

[49] A. Rahimpour, S. S. Madaeni, A. H. Taheri and Y. Mansourpanah, *J. Membr. Sci.*, 2008, **313**, 158-169.

[50] J. Cui, Y. Ju, K. Liang, H. Ejima, S. Lorcher, K. T. Gause, J. J. Richardson and F. Caruso, *Soft Matter*, 2014, **10**, 2656-2663.

[51] S. Kasemset, A. Lee, D. J. Miller, B. D. Freeman and M. M. Sharma, *J. Membr. Sci.*, 2013, **425-426**, 208-216.

[52] S. Herrwerth, W. Eck, S. Reinhardt and M. Grunze, *J. Am. Chem. Soc.*, 2003, **125**, 9359-9366.

Table 1: Membrane properties: water absorption, porosity, and contact angle.

Membrane	Water content (wt. %)	Porosity (%)	Contact angle (θ, degree)	Free energy (-$\Delta G_{SL,}$ mJ m^{-2})
PAN	93.1	51.7	68	100.0
PAN-SiO_2-5%	153.4	64.8	48	121.5
PAN-SiO_2-DOPA-5%	181.5	69.4	40	128.6
PAN-SiO_2-DOPA-10%	202.4	72.1	36	131.7
PAN-SiO_2-DOPA-15%	250.0	77.1	32	134.5

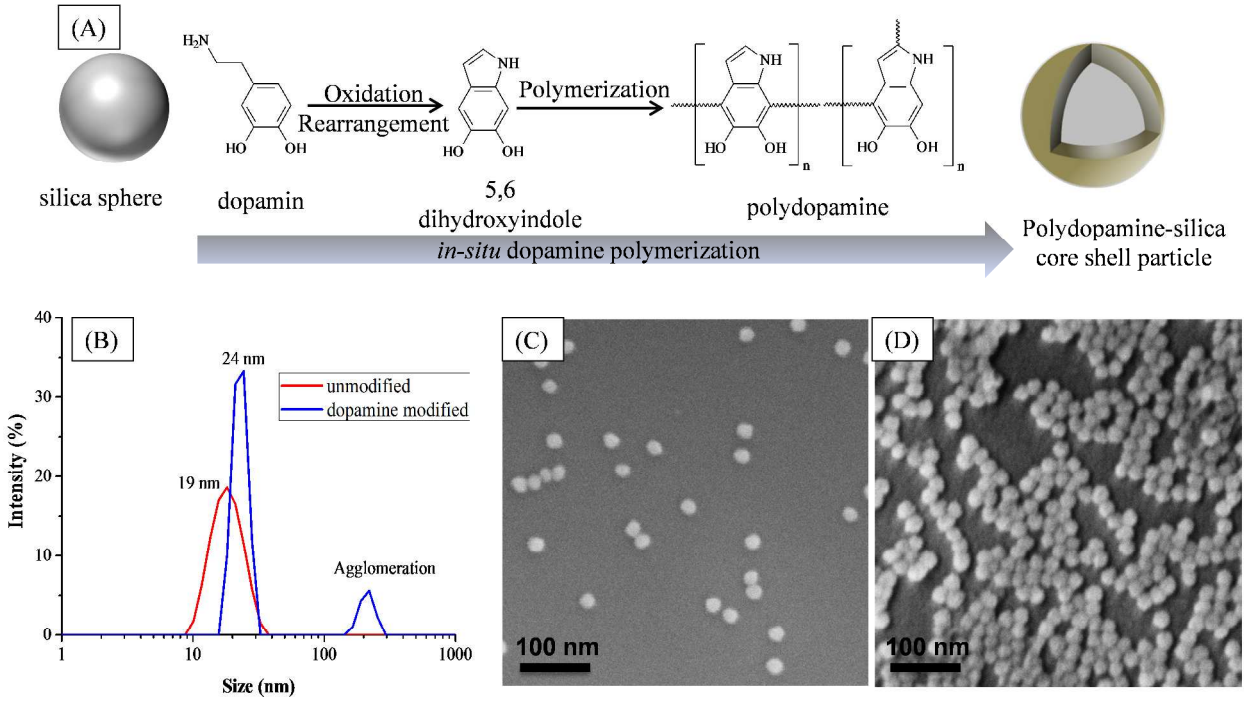

Figure 1. (A) Schematic of polydopamine modification; (B) DLS results; and (C and D) SEM images of dried neat and DOPA modified silica nanoparticles on silicon wafer.

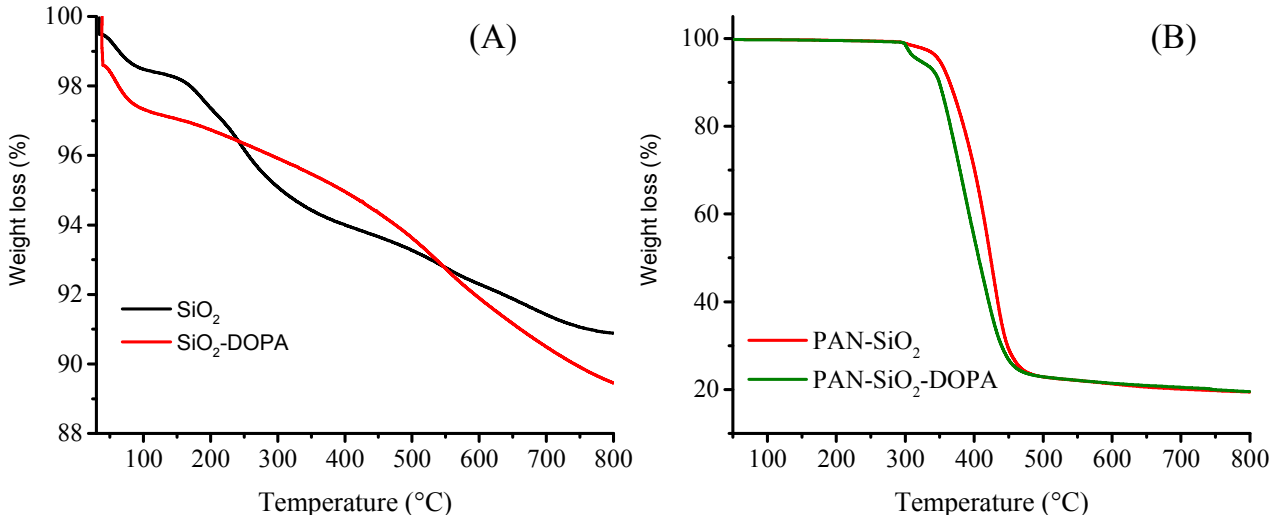

Figure 2: TGA: (A) of neat and DOPA modified silica nanoparticles, and (B) PAN-SiO_2 and PAN-SiO_2-DOPA-15% membranes.

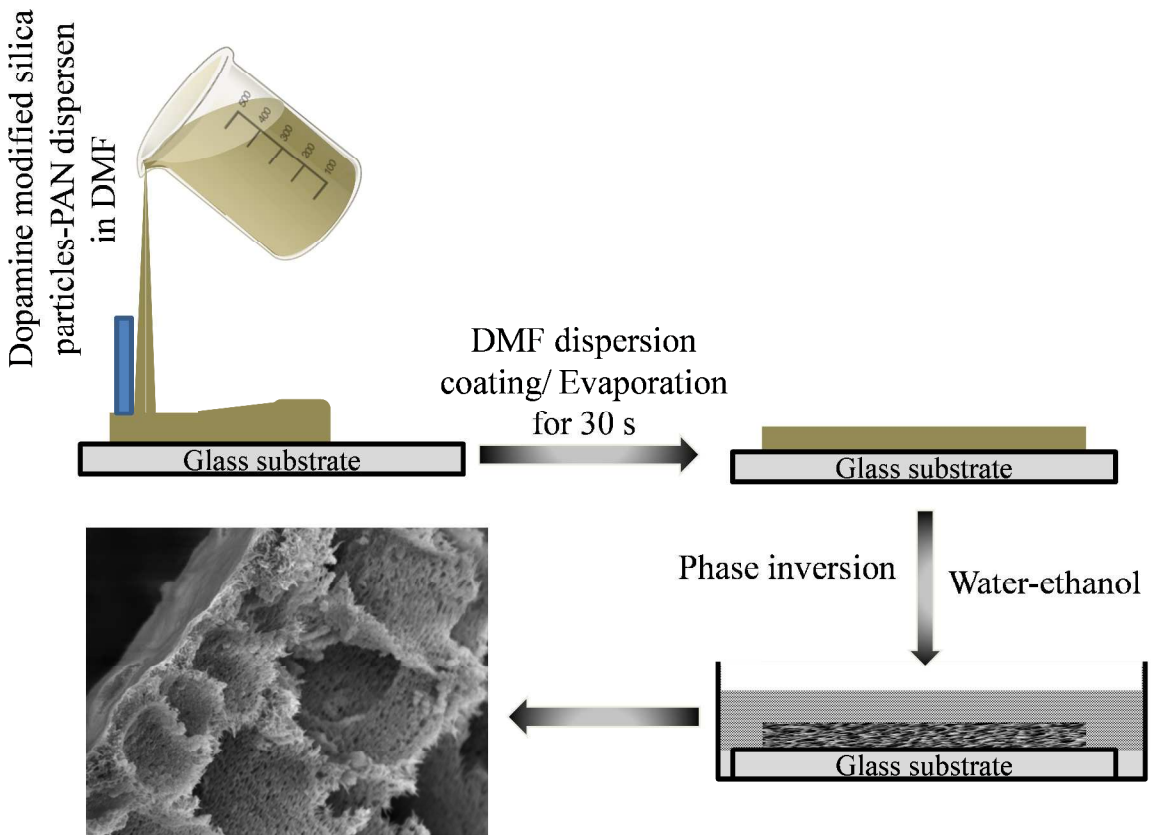

Figure 3. Schematic representation of membrane preparation methodology.

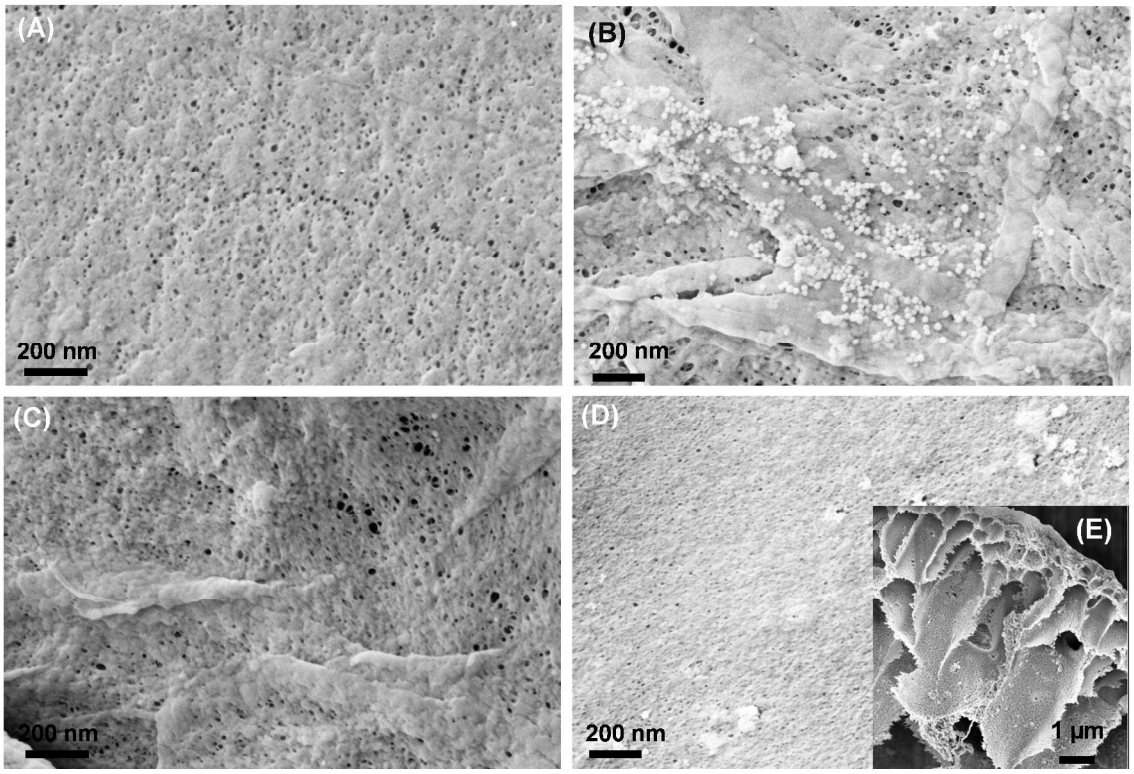

Figure 4. SEM images of membranes: (A) PAN; (B) PAN-SiO_2-5%; (C) PAN-SiO_2-DOPA-5%; (D) PAN-SiO_2-DOPA-10%; and (E) cross-section of PAN-SiO_2-DOPA-10%;

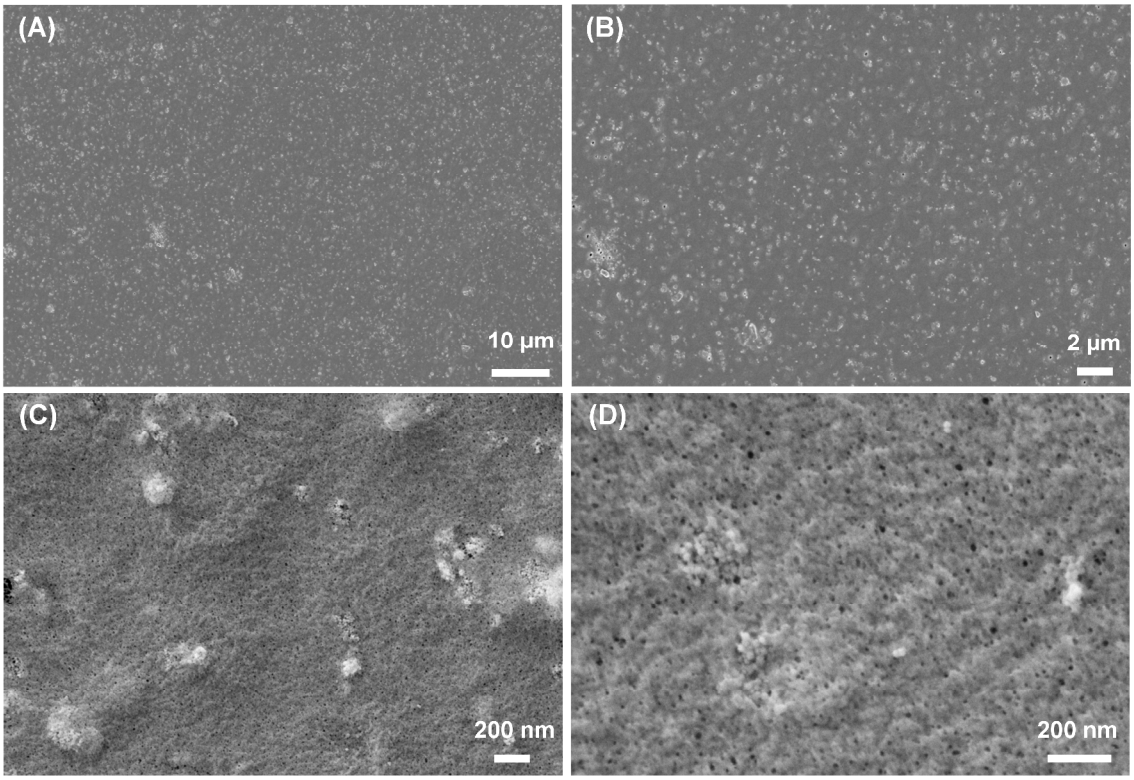

Figure 5. Surface SEM images of PAN-SiO_2-DOPA-15% membrane at different magnification.

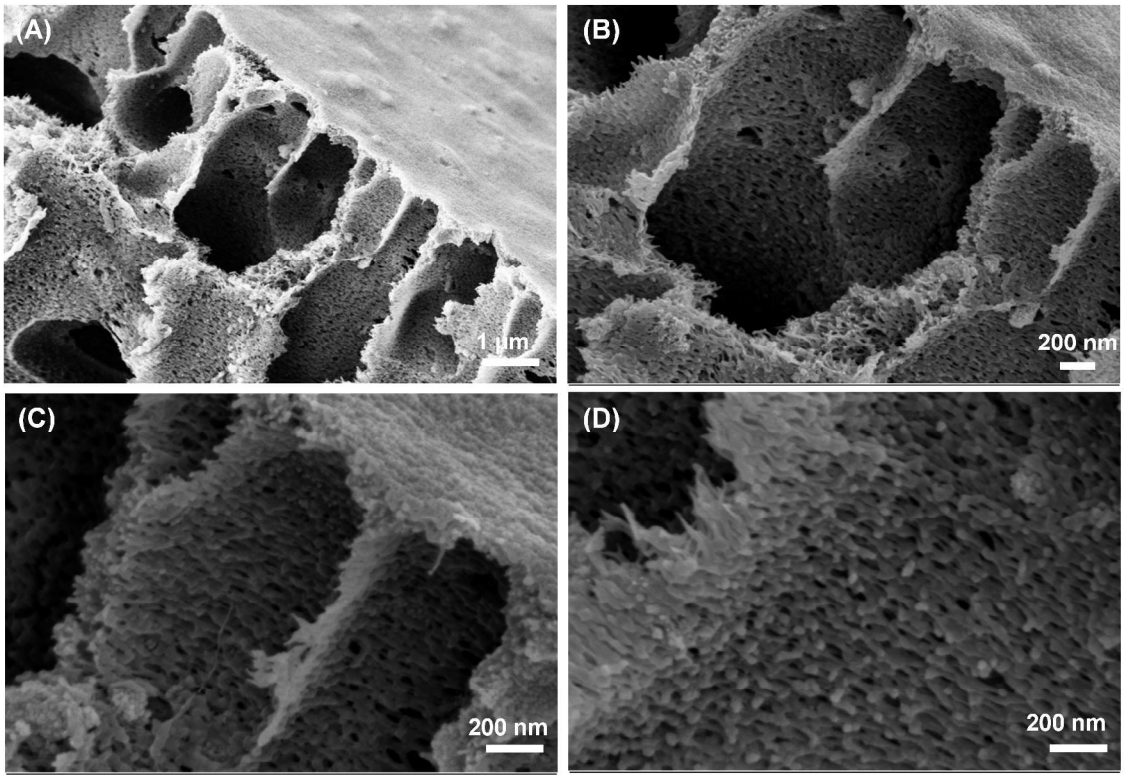

Figure 6. Cross-section SEM images of PAN-SiO_2-DOPA-15% membrane at different magnification.

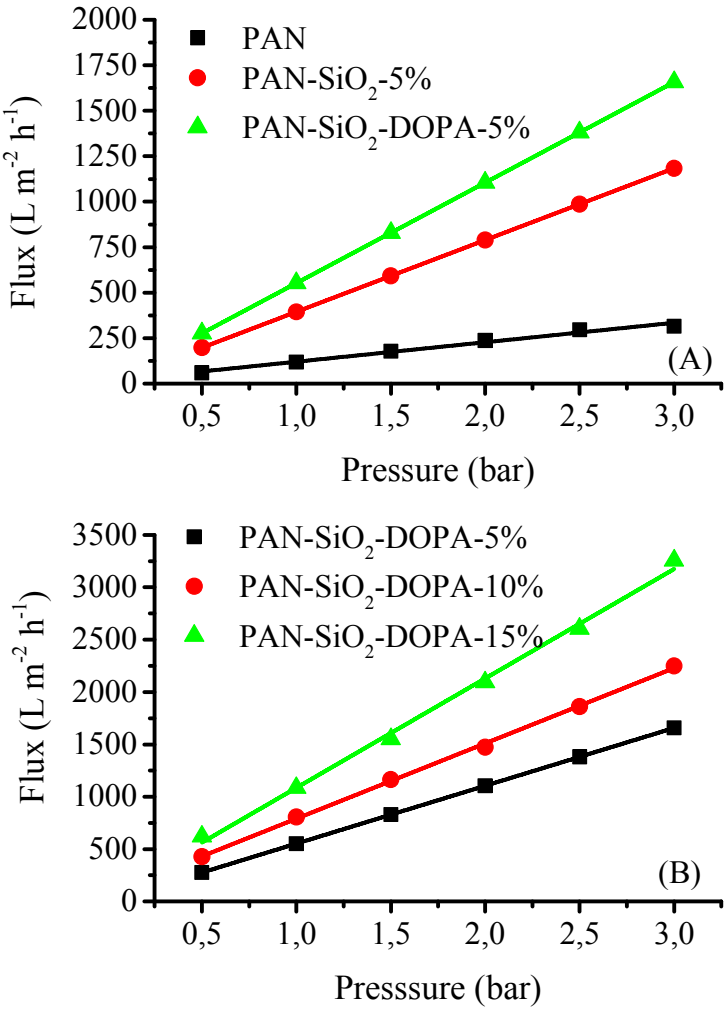

Figure 7. Water permeation properties of different prepared membranes.

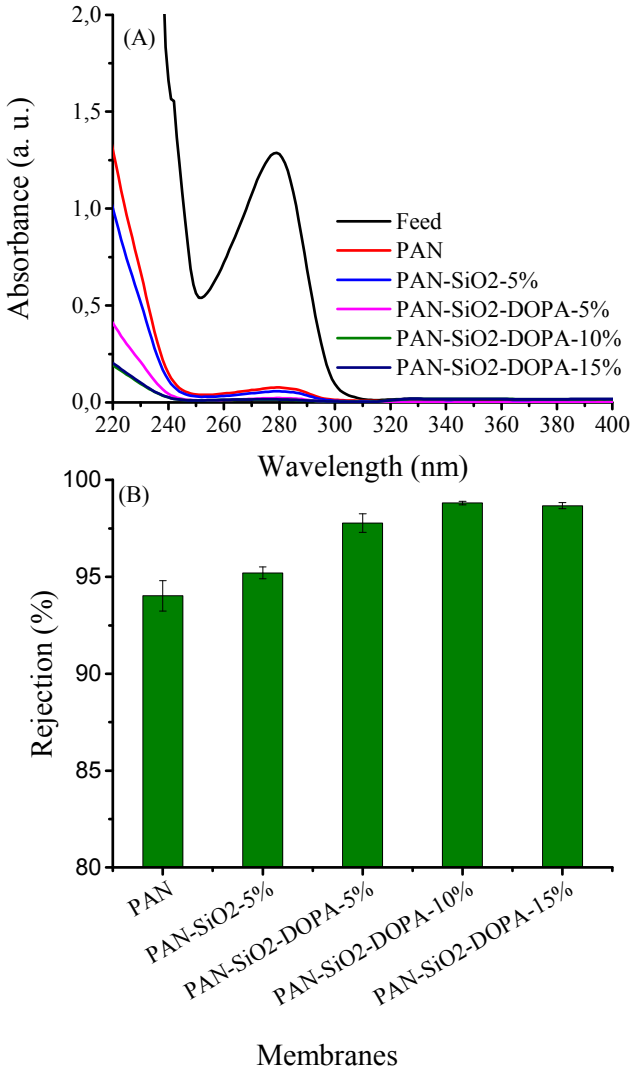

Figure 8. BSA rejection performance of prepared composite membranes: (A) representative UV graphs and (B) percent rejection.

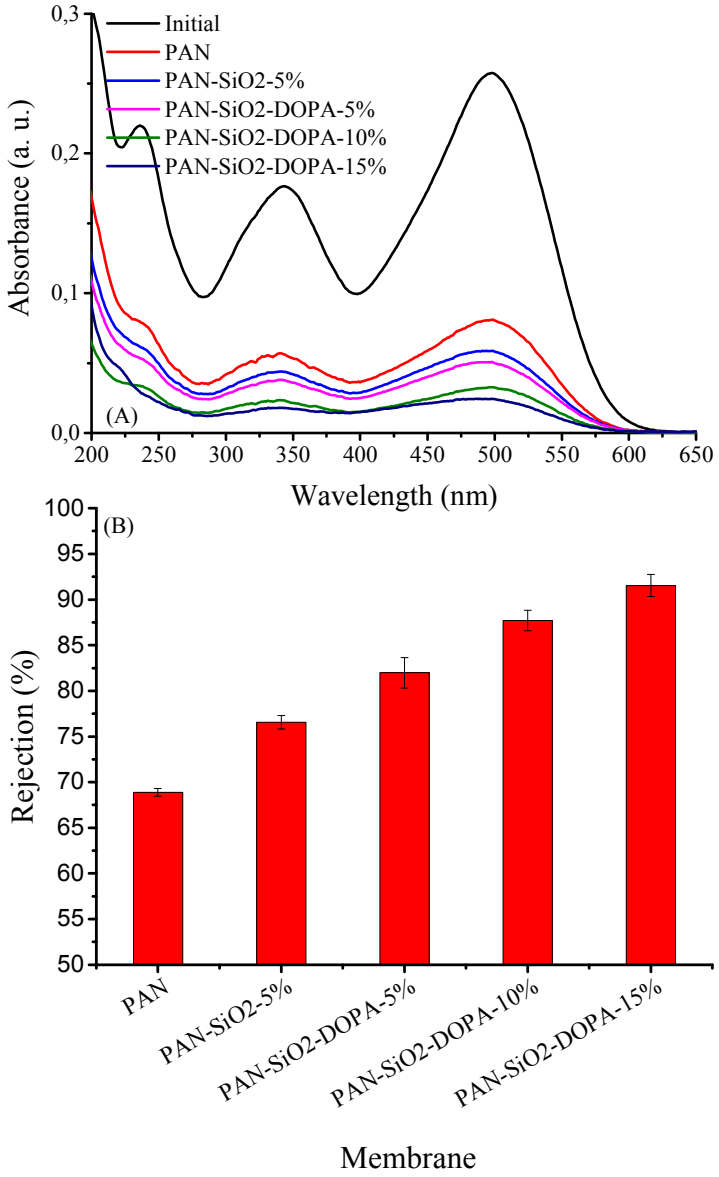

Figure 9. Congo red rejection performance of prepared composite membranes: (A) representative UV graphs and (B) percent rejection.

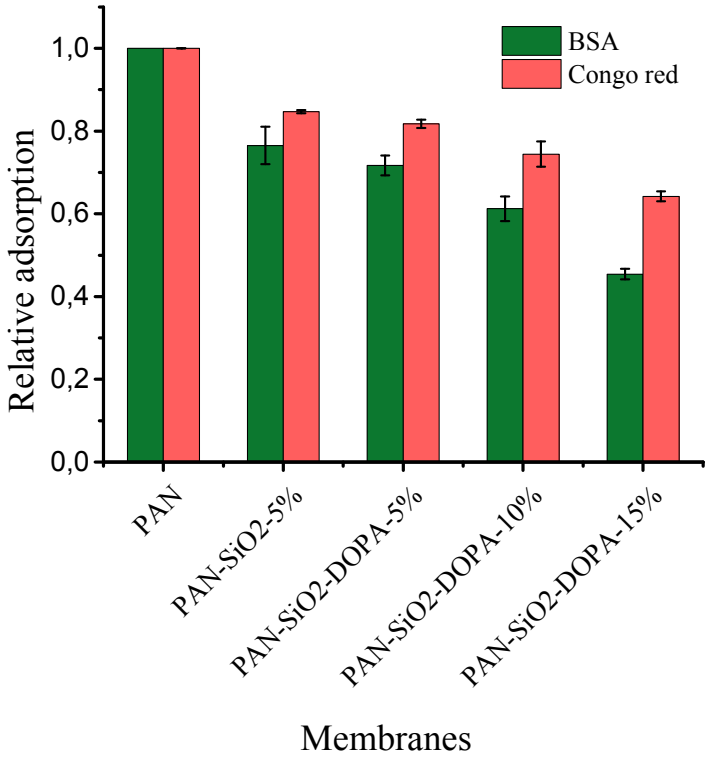

Figure 10. Adsorption experiment of BSA and Congo red dye on membranes.

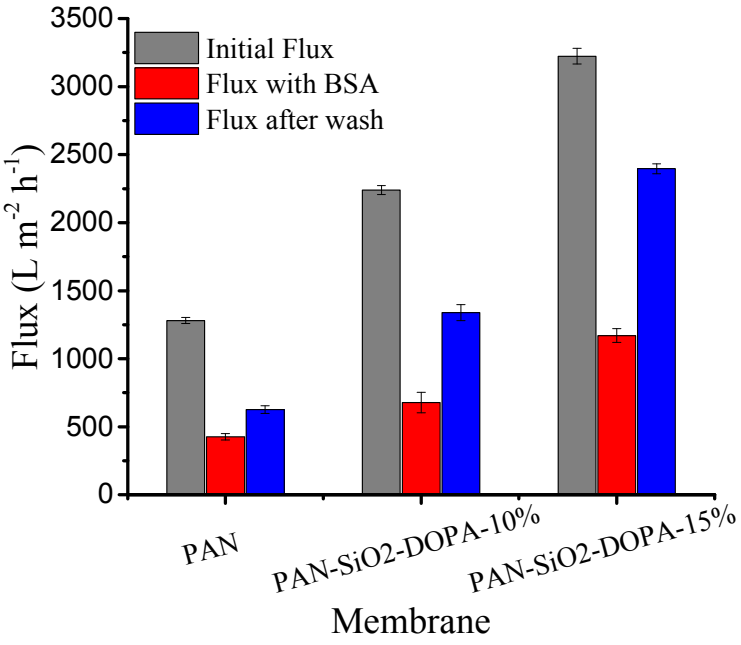

Figure 11. Fouling assessment of the membranes by flux recovery performance after BSA filtration.

TOC

Polydopamine modified silica nanoparticles were incorporated into polyacrylonitrile to fabricate highly hydrophilic and antifouling filtration membranes for water purification applications. High dispersion and better compatibility of polydopamine modified nanoparticles with polyacrylonitrile was observed which resulted into high permeable and rejection membrane.